J Sol-Gel Sci Technol (2013) 65:384–387
DOI 10.1007/s10971-012-2949-6

ORIGINAL PAPER

The (100) orientation evolution and temperature-dependent electrical properties of $Bi(Zn_{1/2}Ti_{1/2})O_3$–$PbTiO_3$ ferroelectric films

Longdong Liu · Ruzhong Zuo · Qian Sun · Qi Liang

Received: 18 November 2012 / Accepted: 21 December 2012 / Published online: 3 January 2013

Abstract The $0.2Bi(Zn_{1/2}Ti_{1/2})O_3$–$0.8PbTiO_3$ (0.2BZT–0.8PT) ferroelectric thin film was successfully fabricated on Pt(111)/Ti/SiO_2/Si substrates by a sol–gel method. The result indicates that the film exhibits the (100) preferred orientation and has a relatively dense and uniform microstructure with a thickness of ~230 nm. The formation mechanism of the oriented films was ascribed to the growth of the (100) oriented PbO layer at ~450 °C during a layer-by-layer crystallization process. Temperature-dependent electrical properties of the 0.2BZT–0.8PT films were investigated, showing that the film has a potential for high temperature applications.

Keywords Sol–gel-preparation · Orientation · Thin films · Temperature dependence · Electrical properties

1 Introduction

Ferroelectric thin films with high Curie Temperatures (T_c) are required for applications in automotive, aerospace, and related industries based on their high electrical performances and good temperature stability [1–3]. $0.36BiScO_3$–$0.64PbTiO_3$ (BS–PT) ceramics and thin films have been investigated in recent years because of their relativity high T_c and good electrical properties [1, 2, 4]. However, the high cost of scandium sources could be an obstacle for the industrial application of BS–PT ceramics and thin films. $Bi(Ni_{1/2}Ti_{1/2})O_3$–$PbTiO_3$ (BNT–PT) systems possess a $T_c > 400$ °C and good piezoelectric properties at the composition of 0.51BNT–0.49PT [5, 6]. $(1-x)Bi(Mg_{1/2}Ti_{1/2})O_3$–$xPbTiO_3$ (BMT–PT) ceramics and thin films also have been reported to have a relatively high T_c (~430 °C) and good electrical properties for the $x = 0.37$ compositions [7–9], while the applications of BNT–PT and BMT–PT systems were limited by their relatively high conductivity and dielectric loss.

$(1-x)Bi(Zn_{1/2}Ti_{1/2})O_3$–$xPbTiO_3$ (BZT–PT) is another member of $BiMeO_3$–$PbTiO_3$ solid solutions with extremely high T_c. Its T_c increases up to 700 °C as the content of BZT increases within the solubility limits [10]. The structural characteristics of BZT–PT ceramics and thin films have been reported by a few groups [11–14], however, their electrical properties have been rarely reported so far. The temperature stability of the electrical properties for ferroelectric thin films is important for practical applications, especially for the electric devices under high temperature environment. Therefore, it is necessary to evaluate the electrical behavior of the BZT–PT thin film as a function of temperature. In this work, the (100) oriented 0.2BZT–0.8PT thin film was fabricated on Pt(111)/Ti/SiO_2/Si substrate by sol–gel method. A focus was placed on the evolution mechanism of the (100) orientation of the 0.2BZT–0.8PT film and the temperature dependence of its ferroelectric properties and leakage current density.

2 Experimental

According to the stoichiometry of 0.2BZT–0.8PT films, 10 mol % excess Pb and Bi were used to compensate for the

L. Liu · R. Zuo (✉) · Q. Sun
Institute of Electro Ceramics and Devices, School of Materials Science and Engineering, Hefei University of Technology, Hefei 230009, People's Republic of China
e-mail: piezolab@hfut.edu.cn

Q. Liang
School of Electronic Science and Applied Physics, Hefei University of Technology, Hefei 230009, People's Republic of China

volatilization loss. Firstly, $Bi(NO_3)_3{\cdot}5H_2O$ (99.0 %) and $Zn(OOCCH_3)_2{\cdot}2H_2O$ (99.0 %) were dissolved in 2-methoxyethanol (2-MOE, 99.0 %) in sequence. $Ti(OC_4H_9)_4$ (98.0 %) was dissolved in 2-MOE with acetylacetone as the stabilizer and chelating agents. $Pb(OOCCH_3)_23H_2O$ (99.0 %) was dissolved in glacial acetic acid. Then, $Pb(OOCCH_3)_2$ solution was added to $Ti(OC_4H_9)_4$ solution and stirred for 10 min. Subsequently, the above mixed solution was added into $Bi(NO_3)_3$ and $Zn(OOCCH_3)_2$ mixed solution and simultaneously stirred to form a stable sol by adjusting the pH value to be ~5.4. Finally, an appropriate amount of *N*, N-Dimethylformamide was added into the above solution to prevent the film from cracking. A little 2-MOE was added to adjust the viscosity and ultimately to form 0.2BZT–0.8PT precursor solution with a concentration of 0.2 M. In order to allow for the test of electrical properties, the $Pt(111)/Ti/SiO_2/Si$ substrates were used for the deposition of the film. After the 0.2BZT–0.8PT precursor solution aged for 3–5 days in air, the thin film was deposited onto $Pt(111)/Ti/SiO_2/Si$ substrates by a repeated spin-coating process at 4,000 rpm for 30 s. After each spin-coating step, the films were dried at 200 °C for 5 min, and pyrolyzed at 450 °C for 8 min under ambient atmosphere. Deposition, drying and pyrolysis processes were repeated for five times and the film was then annealed at 675 °C for 30 min. After that, the above process was repeated for five more times to achieve a desired film thickness (~200 nm). For the electrical measurement, top Ag electrodes of 0.2 mm in diameter were deposited through a shadow mask by means of a thermal evaporation method. The 0.2BZT–0.8PT powder was obtained by drying the precursor solution at 120 °C, and then annealing the xerogel at 675 °C for 30 min.

The phase structures of the film and powder were characterized by an X-ray diffractometer (XRD, D/MAX2500 V, Rigaku, Japan) with Cu Kα radiation. The microstructure on the top surface and fractured cross-section of the 0.2BZT–0.8PT thin film was observed by an atomic force microscope (AFM, Being Nano-Instruments CSPM-4000, Beijing, China) and a field-emission scanning electron microscope (FE-SEM, Sirion200, FEI, Hillsboro, OR), respectively. A ferroelectric testing system (Precision LC, Radiant Technologies Inc., Albuquerque, NM) was used to evaluate the temperature dependence of ferroelectric properties and leakage current density of the BZT–PT thin film.

3 Results and discussion

The XRD patterns of the sol–gel-derived 0.2BZT–0.8PT thin film and powder are shown in Fig. 1. It can be seen that the major peaks of the film could be indexed as a typical perovskite structure except that the (111) diffraction peak was overlapped by the diffraction lines of the substrate. Compared with the diffraction peaks of randomly oriented 0.2BZT–0.8PT powder, the (100) diffraction peak intensity of the 0.2BZT–0.8PT film become significantly enhanced, indicating that the film is (100) preferentially oriented. A Lotgering factor [15] was used to describe the degree of orientation, which was calculated to be 0.84 by using the XRD result in Fig. 1. The evolution of the (100) preferential orientation in the 0.2BZT–0.8PT thin film could be ascribed to the following factors. First of all, the high lead content of the precursor solution might play an important role (10 mol% excess lead). It was reported that the (100) textured PbO thin layer could be easily formed at the interface between the film and substrate [16], which tends to promote the (100) orientation of the 0.2BZT–0.8PT thin films due to their better lattice match. The second reason would be based on the heat treatment condition. The 0.2BZT–0.8PT film was pyrolyzed at 450 °C in this study. Gong et al. [17] found that the $Pb(Zr,Ti)O_3$ (PZT) thin films exhibit (100) orientation as it was pyrolyzed at a temperature of ~450 °C at which the growth of the (100) oriented PbO layer was favored in the amorphous film. On the other hand, Kobayashi et al. [18] explored the effect of multi-spin-coating process on the orientation behavior of PZT thin film. They considered that the PZT film would be (100) oriented as it was crystallized layer-by-layer. On the contrary, only single-crystallization process would result in randomly oriented PZT films. Therefore, the formation of the (100) oriented 0.2BZT–0.8PT film would be also attributed to the layer-by-layer crystallization process in this work because the oriented and thin seed layer can be formed at the interface as it was just crystallized at ~450 °C.

The surface morphology of the 0.2BZT–0.8PT film was examined by AFM, as shown in Fig. 2a. It can be seen that the surface of the film is relatively dense and uniform with

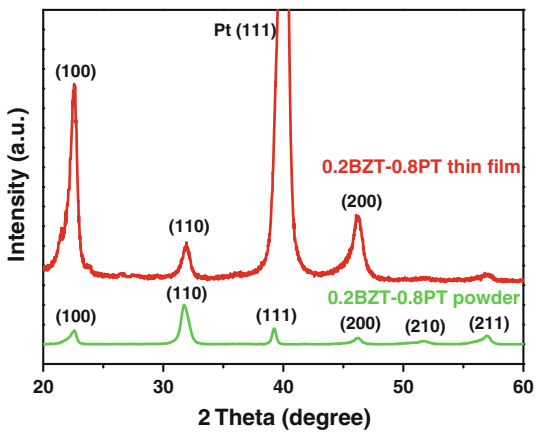

Fig. 1 XRD patterns of the sol–gel-derived 0.2BZT-0.8PT thin film and powder

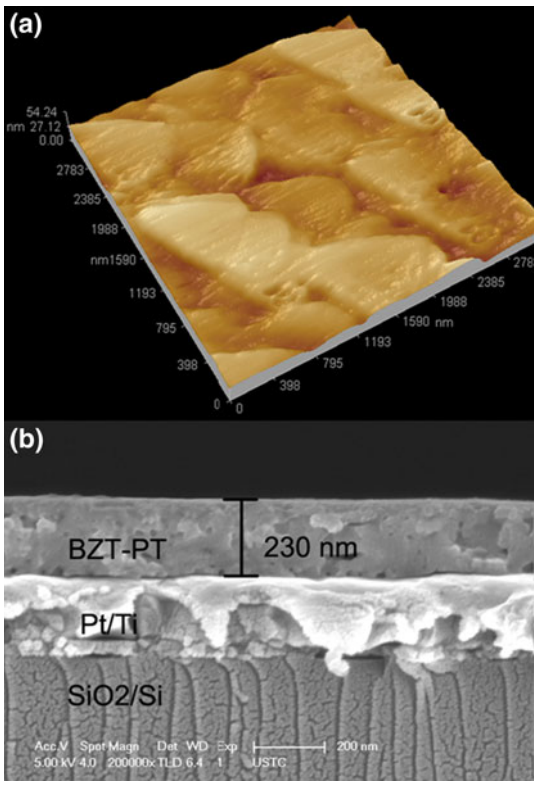

Fig. 2 **a** Surface morphology by AFM and **b** cross-sectional SEM image of the (100) oriented 0.2BZT–0.8PT thin film

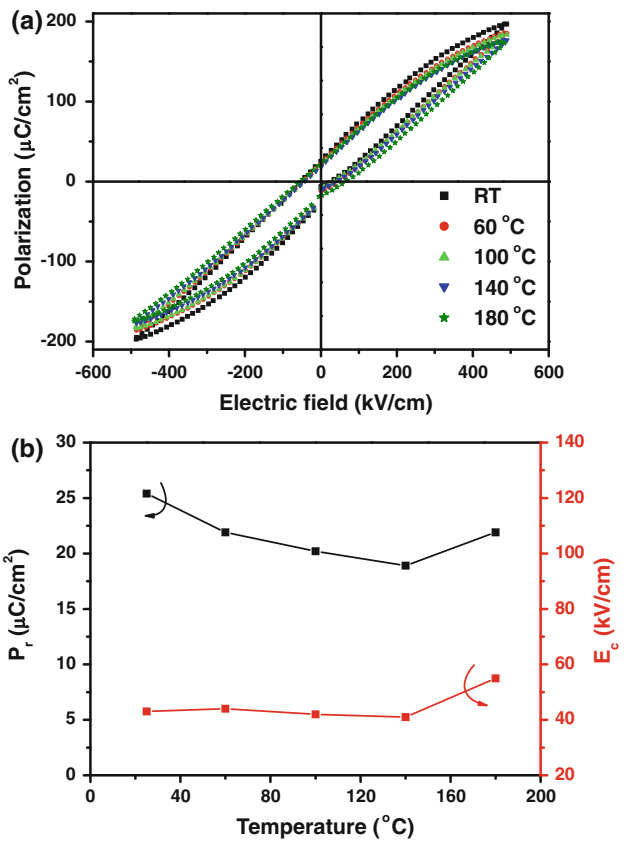

Fig. 3 **a** P–E hysteresis loops and **b** P_r and E_c values as a function of temperature for the (100) oriented 0.2BZT–0.8PT thin film

columnar grains. The microstructure on the fractured cross-section of the film is shown in Fig. 2b. It is obvious that the developed 0.2BZT–0.8PT film looks homogeneous with a thickness of ~230 nm, and stick well to the substrate. No distinct interfaces could be observed between the deposited layers after each spin-coating step. Although the film is well (100) oriented, there is no indication of columnar crystals through the thickness of the layer. Actually this phenomenon has also been found in other works [19, 20]. By comparison, the columnar crystal morphology is usually clear in the film fabricated by pulse laser deposition as a result of the accumulation of plasma.

Temperature-dependent polarization–electric field (P–E) hysteresis loops of the 0.2BZT–0.8PT film at a frequency of 1 kHz are shown in Fig. 3a. It can be observed that the 0.2BZT–0.8PT film exhibits well-defined hysteresis loops at high temperatures. Remanent polarization (P_r) and coercive field $E_c = \left(\left|E_c^+\right| + \left|E_c^-\right|\right)/2$ of the film as a function of temperature are plotted in Fig. 3b. The P_r and E_c values of the thin film at room temperature (RT) are 25.4 μC/cm^2 and 43 kV/cm, respectively. The P_r and E_c values exhibit a slight reduction as the temperature increases from RT up to 140 °C. Since the domain wall motion is a thermally activated process [21], the back-switching of domains would be easier at higher temperatures. It is reasonable to attribute the slight decrease in both P_r and E_c to the increase in the domain wall mobility. However, as the temperature increases to 180 °C, there is a little increase of the P_r and E_c values. This might be due to the increased leakage current at higher temperatures, which would result in nonphysical increase of the P_r and E_c values [22].

Figure 4 displays the electric field dependent leakage current density (J) of the 0.2BZT–0.8PT thin film at various temperatures. It is obvious that the leakage current density increases with increasing the temperature. The value at an applied electric field of 200 kV/cm is 1.2 × 10^{-5} A/cm^2 at RT, and it shows a slight increment to 3.0 × 10^{-5} A/cm^2 at 100 °C. However, it increases rapidly at temperatures higher than 100 °C, reaching to 1.0 × 10^{-4} A/cm^2 at 180 °C. The increased leakage current density at high temperatures would be related to the enhanced activity of the conductivity carriers. The thermal energy generated at high temperatures excited the carriers, making them jump out from the ground state and freely move in the material [23]. The increase in the number of free carriers results in the large leakage current density, which is also responsible for the increase of the P_r and E_c values at 180 °C. These results show that the as-prepared 0.2BZT–0.8PT film has a good thermal stability of electrical properties.

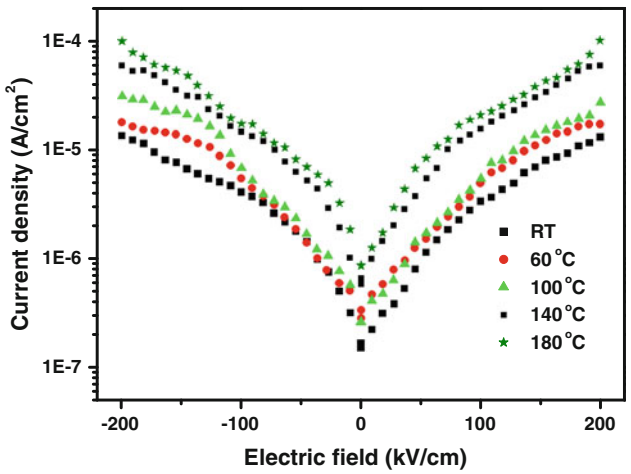

Fig. 4 Leakage current density of the 0.2BZT–0.8PT film as a function of electric field and temperature

4 Conclusions

The (100) oriented 0.2BZT–0.8PT thin film was successfully prepared on Pt/Ti/SiO_2/Si substrate via sol–gel spin-coating method. The AFM and SEM images indicate that a relatively dense and uniform microstructure was obtained and the film thickness was about 230 nm. The 0.2BZT–0.8PT film exhibits well-defined P–E hysteresis loops at high temperatures. The film also shows good electrical resistivity with a leakage current density J $\sim 1.2 \times 10^{-5}$ A/cm^2 under an electric field of 200 kV/cm at RT, however it only slightly increases with increasing the temperature up to 100 °C. These electrical characteristics suggest that the 0.2BZT–0.8PT thin films have potential applications in high temperature ferroelectric devices.

Acknowledgments This work was financially supported by a project of Natural Science Foundation of Anhui province (1108085J14) and the National Natural Science Foundation of China (50972035 and 51272060).

References

1. Yoshimura T, Mckinstry ST (2002) Appl Phys Lett 81:2065–2066
2. Wen H, Wang XH, Zhong CF, Shu LK, Li LT (2007) Appl Phys Lett 90:202902
3. Khan MA, Comyn TP, Bell AJ (2007) Appl Phys Lett 91:032901
4. Eitel RE, Randall CA, Shrout TR, Park SE (2002) Jpn J Appl Phys 41:2099–2104
5. Choi SM, Stringer CJ, Shrout TR, Randall CA (2005) J Appl Phys 98:034108
6. Wu GH, Zhou H, Qin N, Bao DH (2011) J Am Ceram Soc 94:1675–1678
7. Randall CA, Eitel R, Jones B, Shrout TR (2004) J Appl Phys 95:3633–3638
8. Liu LD, Zuo RZ (2011) J Am Ceram Soc 94:3686–3689
9. Liu LD, Zuo RZ, Liang Q. Appl Surf Sci submitted for publication
10. Suchomel MR, Davies PK (2005) Appl Phys Lett 86:262905
11. Grinberg I, Suchomel MR, Dmowski W, Mason SE, Wu H, Davies PK, Rappe AM (2007) Phys Rev Lett 98:107601
12. Zhang XD, Kwon D, Kim BG (2008) Appl Phys Lett 92:082906
13. Kwon D, Kim B, Tong P, Kim BG (2008) Appl Phys Lett 93: 042902
14. Zhong CF, Guo LM, Wang XH, Li LT (2012) J Am Ceram Soc 95:473–475
15. Lotgering FK (1959) J Inorg Nucl Chem 9:113–123
16. Chen SY (1996) Mater Chem Phys 45:159–162
17. Gong W, Li JF, Chu XC, Li LT (2004) J Eur Ceram Soc 24: 2977–2982
18. Kobayashi T, Ichikim M, Tsaur J, Maeda R (2005) Thin Solid Films 489:74–78
19. Zhai JW, Yao X, Xu ZK, Chen H (2006) J Am Ceram Soc 89:354–357
20. Yu Q, Li JF, Zhu ZX, Wang QM (2012) J Appl Phys 112:014102
21. Mihara T, Watanable H (1995) Jpn J Appl Phys 34:5674–5682
22. Meyer R, Waser R (2005) Appl Phys Lett 86:142907
23. Fu F, Zhai JW, X ZK, Ye CG, Yao X (2011) J Mater Sci 46:1053–1057